Soler Cabezas, JL.; Mendoza Roca, JA.; Vincent Vela, MC.; Lujan Facundo, MJ.; Pastor Alcañiz, L. (2018). Simultaneous concentration of nutrients from anaerobically digested sludge centrate and pre-treatment of industrial effluents by forward osmosis. Separation and Purification Technology. 193:289-296. https://doi.org/10.1016/j.seppur.2017.10.058

Simultaneous concentration of nutrients from anaerobically digested sludge centrate and pre-treatment of industrial effluents by forward osmosis

J.L. Soler-Cabezas[1], J.A. Mendoza-Roca[1], M.C. Vincent-Vela[1], M.J. Luján-Facundo[1*], L. Pastor-Alcañiz[2].

[1]Instituto de Seguridad Industrial, Radiofísica y Medioambiental, Universitat Politècnica de València, Camino de Vera, s/n, Valencia 46022 (Spain).

[2]Depuración de Aguas del Mediterráneo (DAM). Avenida Benjamín Franklin, 21. 46980 Parque Tecnológico, Paterna, Valencia (Spain).

Tel. +34963876386

e-mail: malufa@etsii.upv.es

Abstract

In the last years, forward osmosis (FO) has gained increasing prominence, new membranes are being developed and new applications are being considered. In this study, the recovery of nitrogen and phosphorus of the anaerobically digested sludge centrate was studied by FO using two industrial effluents characterized by high osmotic pressure (residual stream from an absorption process for ammonia elimination and brine from a seawater desalination facility) as draw solutions. The experiments were carried

out in a laboratory plant testing two FO membranes (CTA-NW and Aquaporin Inside membrane). Results showed that nitrogen concentration was achieved with both membranes and both draw solutions. The use of the effluent from ammonia absorption enhanced of the nitrogen concentration in the feed stream to the FO membrane. The reached concentration factor in the laboratory tests was 1.61 when Aquaporin membrane was used. Phosphorus could not be concentrated because of its precipitation as calcium phosphate (confirmed by EDX analysis) as a consequence of the high calcium concentration of the municipal wastewater.

Keywords: forward osmosis; draw solution; nutrients concentration; waste water.

1. Introduction

In the last years the recovery of nutrients from wastes and streams coming from sludge treatment processes of municipal wastewater treatment plants (MWWTP) has aroused increasing interest [1]. On the one hand, the recirculation of ammonium nitrogen to the entrance of the MWWTP entails its nitrification increasing the aeration cost. On the other hand, the scarcity of natural sources of phosphorous [2,3] has caused increasing attention to the possibility of phosphorous recovery from streams with high phosphorous concentration like the anaerobically digested sludge centrate (ADSC). In a common wastewater treatment plant, the mixed sludge from primary and secondary treatments is anaerobically digested and then dehydrated by centrifugation. The clarified stream is commonly called ADSC (also called sludge water or sludge liquor from centrifuge).

48 The separated treatment of ADSC began to be studied because of its contribution to the
49 total ammonium nitrogen entering the biological reactor, which makes difficult the
50 accomplishment of the legal nitrogen discharge standard [4]. In fact, the nitrogen load
51 of this stream could contribute to the total nitrogen entering the wastewater treatment
52 plant (WWTP) up to 25% [5,6]. Thus, the main characteristic of this stream is its high
53 ammonium nitrogen concentration, which can be higher than 1000 $mg \cdot L^{-1}$. In addition
54 to it, the concentration of phosphorous is also high [7], around 8% of the phosphorous
55 load entering the plant, as reported by Holloway et al. [8]. In this way, Ping et al. [9]
56 proposed recently a separated treatment consisting of a reactor for precipitating it in
57 struvite form in order to recover phosphorous from the ADSC. They published that
58 amorphous calcium phosphate (predominant with low PO_4-P precipitates), calcite,
59 brucite (predominant with high PO_4-P precipitates) and magnesium phosphate were also
60 precipitated.

61 Most of the works that can be found in the literature proposing the separated treatment
62 of the ADSC suggest eliminating the nitrogen biologically without taking into account
63 the possibility of its recovery for a further agricultural use. Thus, a separated biological
64 treatment based on the Single reactor system for High
65 activity Ammonium Removal Over Nitrite (SHARON) processes [10] was even
66 implemented at industrial scale [11] and deeply studied by other authors [12]. Fux et al.
67 [12] studied nitrogen removal by nitration/denitritation process by means of a
68 sequencing bath reactor (SBR) operating with continuous dewatering liquor addition.
69 Results showed that around 85-90% nitrogen was removed. Biological nitrogen
70 elimination through nitrite saves aeration costs since the oxidation of nitrite to nitrate
71 was avoided. Furthermore, the combination of SHARON and anaerobic ammonium
72 oxidation (ANAMMOX) processes [10] could reduce the costs even more; since nitrites

are reduce by the ammonium-nitrogen in this process. However, a solution including nitrogen recovery instead of nitrogen elimination is undoubtedly better from an economical and an environmental point of view.

In the last years, forward osmosis (FO) has gained increasing prominence, new membranes are being developed and new applications are being considered [13]. Thus, applications of this technique can be found in the literature. For example, Holloway et al. [8] studied nutrients removal by FO from anaerobic digester centrate combining with a reverse osmosis (RO) process. They found that at larger-scale approximately the 70% of water was recovered (results from mathematical model). FO allows concentrating one liquid stream diluting another one simultaneously. According to the article review about hybrid FO processes by Checkly et al. [14], the key of the success of the application lies on avoiding an expensive further treatment of the diluted draw solution (DS) for its regeneration or on finding an economically feasible hybrid process [14]. Van der Bruggen and Luis [15] and Shaffer et al. [16] published interesting critical reviews about the FO process and its applications. There is a lack of works of the literature that report FO processes using industrial effluents as DS. Only the work performed by Duan et al. [17] is cited in these review papers. These authors proposed the use of sodium lignine sulfonate (a residual stream of the paper manufacturing). The diluted draw solution was applied directly as a medium for plant growth in deserts [17]. The use of actual industrial effluents has the great advantage that they have not to be regenerated.

The selection of the DS is of great importance, since the concentration difference of the compounds between feed and draw sides enhances the reverse salt flux by the Fick's law [18]. In this way, the increment of the ions concentration in the feed solution has to be previously taken into account. In this way, studies about direct and reverse salt passage through FO membranes using model solutions can be found in the literature

[19–21]. Hancock et al. [19] reported that the specific reverse salt flux in FO processes ranges between 80 and 3000 $mg \cdot L^{-1}$ stating that monovalent ions had lower range of permeation than divalent ions. Philip et al. [20] noticed that the reverse salt flux was independent of the DS concentration and the structure of the membrane support layer. Holloway et al. [21] reported that the RSF was lower for mixed salts DSs than for pure NaCl solutions.

Until now, the treatment of the ADSC by FO has hardly been studied. Table 1 summarizes these previous studies. For example, Ansari et al. [7] used FO for recovering the phosphorous by precipitation, since the progressive pH increase in the ADSC used as feed solution enhanced the separation of the phosphorous by precipitation. However, any of these studies uses actual industrial wastewater as DS.

In this work, the concentration process by FO of nitrogen and phosphorus in the anaerobically digested sludge centrate was studied using two industrial effluents characterized by high osmotic pressure (residual stream from an absorption process for ammonia elimination and brine from a seawater desalination facility) as draw solutions. The behavior of two FO membranes were compared both in terms of the permeate flux and in terms of reverse salt flux for the aforementioned application.

Table 1: Previous studies about the treatment of the ADSC by FO.

Year	Membrane	Feed Solution	Draw solution	Concentration rate	Reference
2007	CTA-HTI	Raw and filtered centrate	NaCl solution (70 $g \cdot L^{-1}$)	high retentions of orthophosphate (higher than 99.5%) and ammonia (between 85 and 91.6%)	[8]
2016	CTA-HTI	Digested Sludge Centrate	See water	95% of the initial phosphate	[7]
2017	Aquaporin Inside	Synthetic digestate	NH_4HCO_3 solution	Recover the 99,7% of ammonium nitrogen and 79,5% of phosphorous	[22]
2018	CTA-HTI	Municipal sewage	NaCl solution	Sewage concentration up to 90%	[23]

116 **2. Material and methods**

117

118 2.1. Feed solutions

119 Two feed solutions (FS) were used for each DS tested in the FO experiments. The first
120 FS was deionized water with a conductivity value lower than 10 $\mu S \cdot cm^{-1}$. The second
121 one was the ADSC from a municipal wastewater treatment plant located near Valencia
122 (Spain). All the ADSC samples have been taken from the outlet pipe of the centrifuge,
123 which works at 3000 rpm. The ADSC pre-treatment before each FO test consisted of
124 filtering the sample with a 500 microns mesh. After this pre-treatment, the ADSC was
125 characterized and results were shown in Table 2.

126 It has to be highlighted the great variability of the values of total phosphorous (TP),
127 chemical oxygen demand (COD) and suspended solids (SS) in comparison with pH,
128 conductivity, total nitrogen (TN), ammonium nitrogen (NH_4-N) and calcium (Ca^{+2}),
129 whose standard deviations are in a much lower percentage. The explanation for the SS
130 variability lies on the efficiency of the centrifugation process. In addition to it, a slight
131 increase in the ADSC suspended solids concentration will also entail an increase in the
132 total COD of the sample. Concerning to the phosphorous variability, this fact may be
133 due tospontaneous calcium phosphate and struvite precipitation occurring at the
134 anaerobic digester exit. The uncontrolled struvite precipitation was recently estimated
135 by Martí et al. [24] in 9.5 g of TP per kg of sludge.

136

137

138

139 **Table 2: Characterization of the CADS used in the FO experiments as FS (number of samples = 5).**

Parameter	Value
pH	8.1 ± 0.2
Conductivity ($mS \cdot cm^{-1}$)	9.69 ± 1.50
COD ($mg \cdot L^{-1}$)	1,941 ± 837
SS ($mg \cdot L^{-1}$)	559 ± 343
TN ($mg \cdot L^{-1}$)	975 ± 164
NH_4-N ($mg \cdot L^{-1}$)	886 ± 189
TP ($mg \cdot L^{-1}$)	10.4 ± 8.1
Ca^{2+} ($mg \cdot L^{-1}$)	203 ± 25
Mg^{2+} ($mg \cdot L^{-1}$)	114 ± 29
SO_4^{2-} ($mg \cdot L^{-1}$)	110 ± 37
Cl^- ($mg \cdot L^{-1}$)	1,412 ± 301
Na^+ ($mg \cdot L^{-1}$)	417 ± 102
K^+ ($mg \cdot L^{-1}$)	388 ± 41
Osmotic pressure (bar)	5.3

140

141 2.2. Draw solutions

142 Two DS were used in the FO tests: brine from seawater desalination taken in a plant
143 located in Alicante province (Spain) and the liquid effluent from an absorption process
144 for ammonia removal taken in an industrial wastewater treatment plant located in
145 Galicia (Spain). The absorption liquid effluent (ALE) consisted basically of ammonium
146 sulfate since sulfuric acid was employed for ammonia recovery coming from a
147 desorption process. Thus, the characterization of the ALE has been carried out in terms
148 of pH, conductivity, NH_4-N and sulfates (SO_4^{-2}) concentration. Table 3 shows the
149 composition of the brine and the ALE samples used in the experiments. The pH of the
150 ALE was increased up to 7.0 (with NaOH 40% w/w, from Panreac, Spain) so that
151 membranes could not be damaged by the acidic pH. The molarity values of the sodium
152 chloride in brine and the molarity of the ammonium sulfate in ALE were 1.2M and 1 M,
153 respectively. These values were calculated on the basis of the chloride and ammonium-
154 nitrogen measured concentration, respectively.

155

156 **Table 3: Characterization of the DS used in the experiments.**

Parameter	ALE	Brine
Conductivity ($mS \cdot cm^{-1}$)	152	84.7
SO_4^{2-} ($mg \cdot L^{-1}$)	154,500	5,750
NH_4-N ($mg \cdot L^{-1}$)	28,618	----
Cl^- ($mg \cdot L^{-1}$)	----	43,850
Na^+ ($mg \cdot L^{-1}$)	----	23,000
Ca^{2+} ($mg \cdot L^{-1}$)	----	2,475
Mg^{2+} ($mg \cdot L^{-1}$)	----	3,075
K^+ ($mg \cdot L^{-1}$)	----	740
Osmotic pressure (bar)	76	54

157

158

159 2.3. Analytical methods

160 The characterization of the draw and feed solutions included the analysis of the
161 following ions: NH_4^+-N, Ca^{+2}, magnesium (Mg^{+2}), SO_4^{-2}, chloride (Cl^-), potassium (K^+)
162 and sodium (Na^+). NH_4^+-N content was determined by a "Pro-Nitro M" distiller (P-
163 Selecta, Spain). Ca^{+2}, Mg^{+2}, SO_4^{-2}, Cl^- and K^+ concentrations were measured using kits
164 and the spectrophotometer NOVA 30 both provided by Merck (Spain). The Na^+
165 concentration was analyzed by means of sodium selective electrode ISE IntelliCAL HQ
166 40d supplied by Hach Lange (Spain). All of these parameters were analyzed after
167 filtering the samples with a 60 μm filter.

168

169 pH and conductivity measurements were carried out with pHMeter GLP 21+ and EC-
170 Meter GLP 31+ (CRISON), respectively. Total solids (TS) were measured according to
171 Standard Methods [25]. COD, TN, and TP were analyzed using kits and the
172 spectrophotometer DR600, both provided by Hach Lange (Spain).

173

174 2.4. Laboratory plant

175 Experiments were carried out in a laboratory plant (Fig. 1) equipped with a CF042-FO
176 module (STERLITECH, USA) that could house a flat sheet membrane with an active
177 surface of 42 cm^2. In order to measure continuously the conductivity of the feed and
178 draw solutions, two conductivity meters (model CDH-SD1 from Omega Engineering,
179 United States) trademark was used in the tests performed. The draw and the feed
180 solutions were pumped to the module by two peristaltic pumps, Pumpdrive 5106
181 (HEIDOLPH, Germany). The flow rate of the draw and the feed solutions were
182 measured with flow meter 2300 from TECFLUID (Spain) and was adjusted to 30 $L \cdot h^{-1}$.

183 The mass of water that passes through the membrane was measured from the mass
184 change of the draw solution tank. For it, a digital scale model PKP from KERN
185 (Germany) was used. It can measure up to 4,200 g with a maximum deviation of 0.01 g.
186 The measurements were registered every minute in a computer with a RS232 to USB
187 cable and the software "Kern Balance Connection SCD-4.0".

188

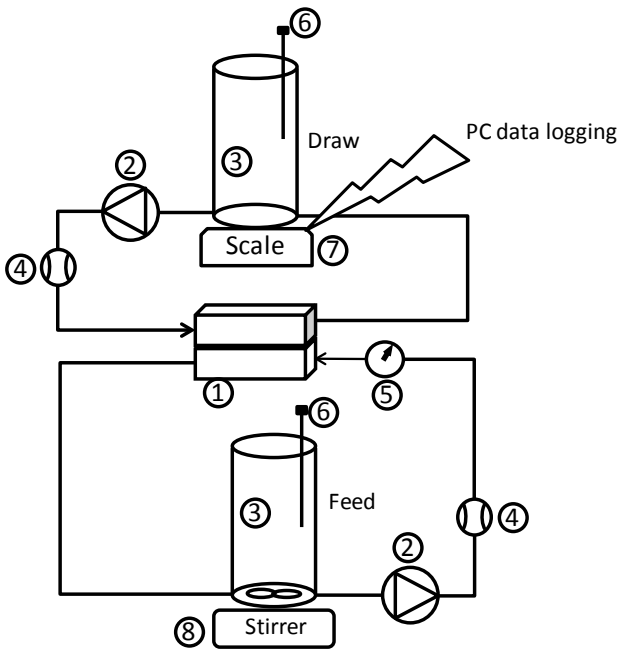

189

190 **Figure 1: Scheme of the laboratory-scale plant. (1) forward osmosis module, (2) peristaltic pump, (3) Tank, (4)**
191 **flow meter, (5) pressure gauge, (6) conductivity meter, (7) scale, (8) magnetic stirrer.**

2.5. Membranes and experimental planning

Two flat sheet membranes were used in the experiments: CTA-NW from HTI (USA) and Aquaporin INSIDE™ (AIM) from AQUAPORIN A/S (Denmark). The tests were carried out with the active layer of the membrane facing the feed solution. After each FO experiment, the membrane was cleaned out of the module. It was submerged in a solution with EDTA (0.8% w/v) and Alconox (1% w/v) during 1 hour and the pH of this solution was corrected until reaching a pH value of 6.6.

All the experiments followed the same methodology. The duration was 72 hours. Conductivity of draw and feed solutions and mass of the DS were measured continuously. The analysis carried out depended on the DS and the FS tested. Nine experiments were carried out. They are detailed in Table 4.

Before and after each test, membrane was characterized by determining its permeability and its salt reverse flux as it was detailed in a previous study [18]. The membrane water flux (J_w) was calculated following Eq. 1:

$$J_w = \frac{\Delta V}{A \cdot \Delta t} \quad (1)$$

Where, ΔV is the total volume increase in the draw solution tank (L) in a Δt (h) period, and A is the active FO membrane area (m^2). The specific reverse salt flux (SRSF) expressed in $mg \cdot L^{-1}$ in the FO experiments has been calculated according to Eq. 1. Several authors like Nguyen et al. [26] and Zou et al. [27] also calculated the SRSF as it is showed in Eq. 2.

213 $$SRSF = \frac{V_{F,f} \cdot C_{F,f} - V_{F,i} \cdot C_{F,i}}{V_{F,i} - V_{F,f}} \quad (2)$$

214

215 Where $V_{F,f}$ is the feed volume at the end of the FO experiment, $C_{F,f}$ is the ion
216 concentration in the feed at the end of the experiment, $V_{F,i}$ is the feed volume at the
217 beginning of the FO experiment (t = 0) and $C_{F,i}$ is the ion concentration in the feed at
218 the beginning of the experiment (t = 0).

219 Membranes samples before and after the FO tests with ADSC as FS were also observed
220 with a Field Emission Scanning Electron Microscopy (FE-SEM) model Ultra 55 from
221 Oxford Instruments (United Kingdom). Elemental analysis was also carried out to find
222 out the composition of the precipitated salts.

223

224 **Table 4: Experimental planning for the FO tests.**

Test number	Membrane	FS	DS
1	CTA-NW	Deionized water	ALE
2	CTA-NW	ADSC	ALE
3	CTA-NW	Deionized water	Brine
4	CTA-NW	ADSC	Brine
5	AIM	Deionized water	Brine
6	AIM	ADSC	Brine
7	AIM	Deionized water	ALE
8	AIM	ADSC	ALE

225

226

227

228

229

230

231 **3. Results**

232

233 3.1. Characterization of the pristine membranes

234 Fig. 2.a shows the permeability of both membranes used. The water flux values at
235 different NaCl concentrations in DS (FS was deionized water) can be compared. The
236 represented values correspond to the mean permeate fluxes of the four characterization
237 tests. Standard deviations have also been included. It can be observed that the permeate
238 flux of AIM increases much more with the NaCl concentration in DS than the permeate
239 flux of the CTA-NW membrane. In fact, the permeate flux of the CTA-NW membrane
240 was the highest at 25 $g \cdot L^{-1}$ of NaCl. At 100 $g \cdot L^{-1}$ of NaCl, the permeate fluxes of both
241 membranes were very similar, while the permeate flux of the AIM was clearly the
242 highest one at 200 $g \cdot L^{-1}$ of NaCl.

243 Fig. 2.b illustrates the reverse salt flux (J_s) of the pristine membranes as a function of
244 the NaCl concentration in the DS. J_s was practically the same at the minimal salt
245 concentration (25 $g \cdot L^{-1}$), meanwhile the reverse salt flux was the highest for the AIM
246 when increasing salt concentration. This is in concordance with the high J_w values at
247 high NaCl concentrations.

248 In relation with the Js/Jw ratio, the lowest result was obtained for the CTA-NW (mean
249 value = 0.47 $g \cdot L^{-1}$). That means that there will have a lower specific reverse salt flux
250 when this membrane is used in comparison with the AIM, whose mean Js/Jw ratio was
251 0.6 $g \cdot L^{-1}$. From the Jw and Js data the parameters A (water permeability coefficient) and
252 B (solute permeability coefficient) have been calculated according to an Excel-based
253 error minimization algorithm developed by Tiraferri et al. [28]. The mean values,

254 considering four permeability tests, were A = 0.235 $L \cdot m^{-2} \cdot h^{-1} \cdot bar^{-1}$ and B = 0.095 $L \cdot m^{-2} \cdot h^{-1}$ for the

255 CTA-NW membrane and A = 0.231 $L \cdot m^{-2} \cdot h^{-1} \cdot bar^{-1}$ and B = 0.081 $L \cdot m^{-2} \cdot h^{-1}$ for the AIM.

256

257 a)

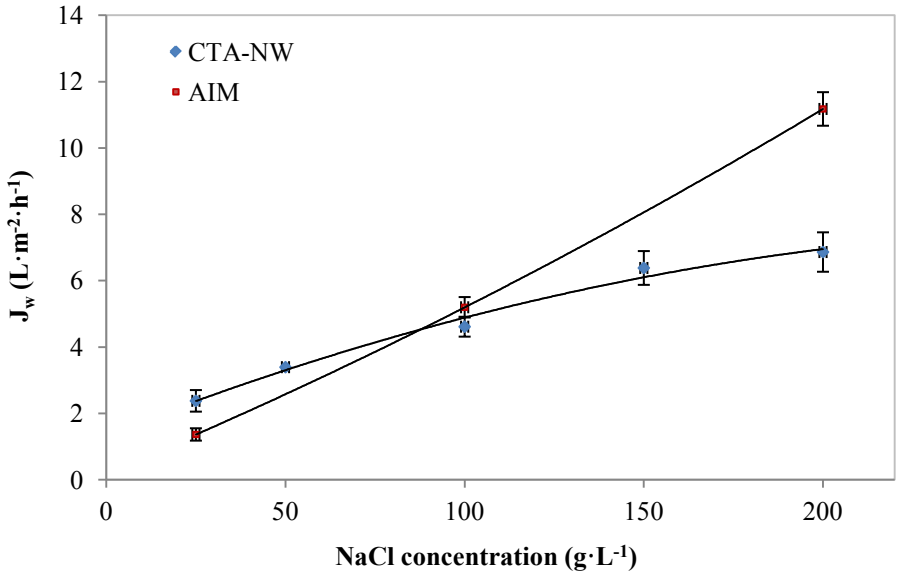

258

259 b)

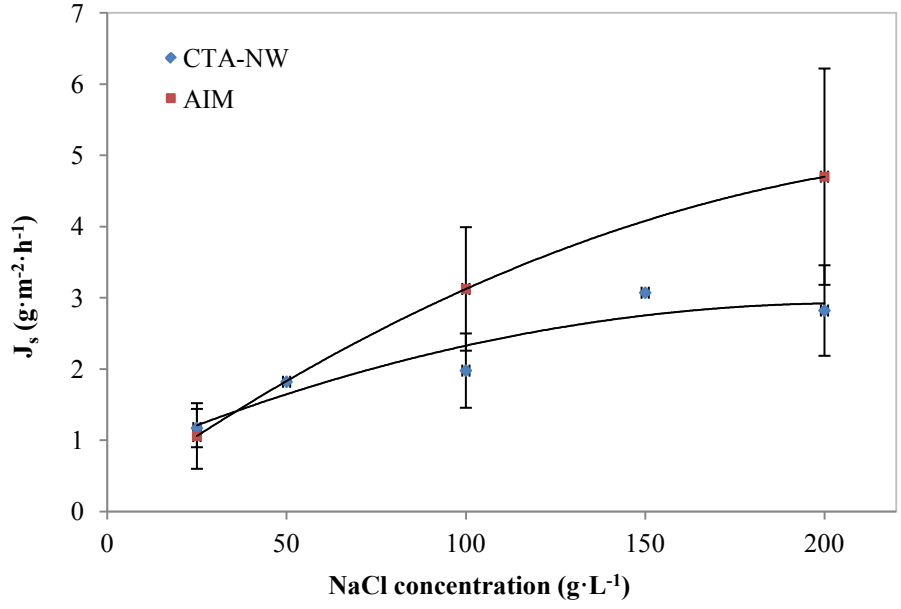

260

261 **Figure 2: a) Water flux of the pristine membranes and b) reverse salt flux of the pristine membranes.**

262

263 3.2. Tests using deionized water as feed solution

264 Comparison in terms of permeate water flux

265 Fig. 3 shows the permeate water fluxes measured in the experiments using deionized
266 water as FS for the ALE (Fig. 3.a) and the brine DS (Fig. 3.b). It can be observed that
267 the measured fluxes in the tests with AIM were higher than those measured in the tests
268 with the CTA-NW membrane. This is in concordance with the results of the
269 permeability experiments explained in section 3.1. However, the water flux difference
270 between the membranes decreased during the experiments. It can be explained by the
271 faster diminution of the driving force in the case of the AIM, since the water drawn
272 volume was higher than in the case of the CTA-NW membrane.

273 In the tests with ALE as DS, the final permeate water fluxes were 3.56 and 3.13 $L \cdot m^{-2} \cdot h^{-1}$ for
274 the AIM and CTA-NW, respectively. The final flux values in the experiments with
275 brine as DS were 3.34 and 2.92 $L \cdot m^{-2} \cdot h^{-1}$ for AIM and CTA-NW, respectively. In other
276 words, practically the same flux difference in favor of AIM was achieved irrespective of
277 the DS.

278

279 a)

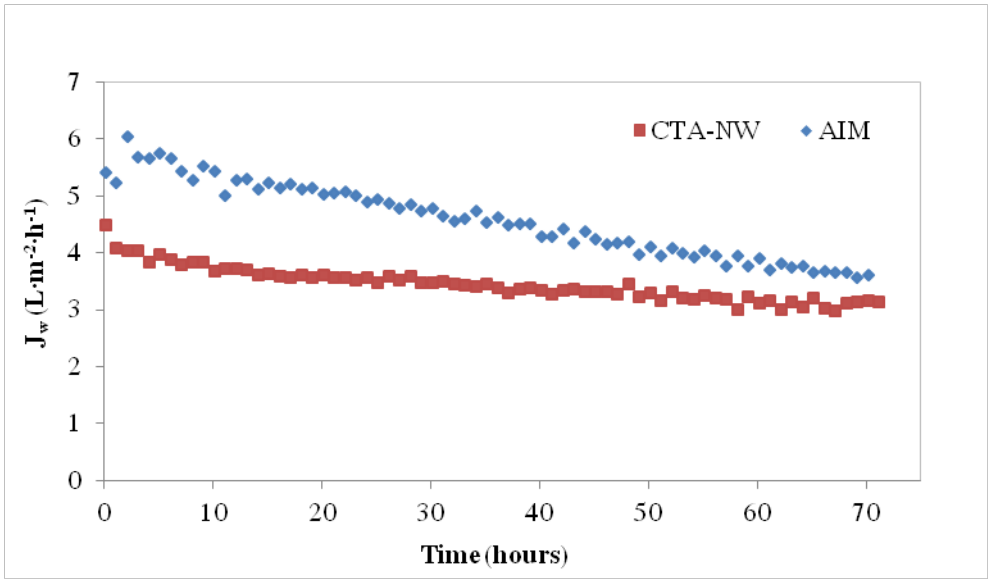

280

281 b)

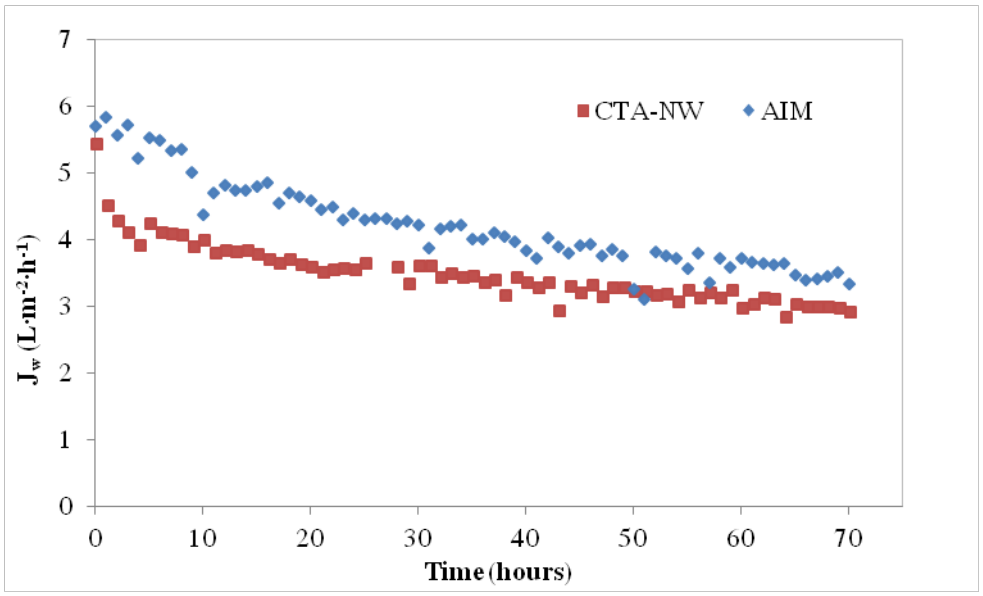

282

283 **Figure 3: Flux evolution in the tests with deionized water as FS and**
284 **a) ALE as DS and b) brine as DS.**
285

286

287

288

289

290 Comparison in terms of specific salt reverse flux

291 Fig. 4 shows the specific reverse fluxes of the ions using ALE (Fig. 4.a) and brine (Fig.
292 4.b). As the FS was deionized water (conductivity lower than 10 $\mu S \cdot cm^{-1}$), it was
293 assumed that the ions concentration in the feed at the beginning of the experiments
294 ($C_{F,i}$) were negligible.

295 In the case of ALE (Fig. 4.a), the SRSF for sulfate was 9.7% higher in the experiment
296 with the AIM than in the test with CTA-NW membrane. However, the NH_4-N reverse
297 flux was lower in the case of using the AIM. It can be explained by the direct NH_4-N
298 passage (from FS to DS) during the test, which diminishes the final reverse flux
299 obtained. In other words, it indicates that the ammonium-nitrogen rejection by the AIM
300 was lower than that of the CTA-NW membrane. This point will be further discussed in
301 section 3.3.

302 Nasr and Sewilam [29] used ammonium sulfate solutions of a wide concentration range
303 as DS in a FO process. These authors reported considerably higher SRSF than those
304 measured in this work. In fact, for permeate water fluxes between 5 and 10 $L \cdot m^{-2} \cdot h^{-1}$,
305 reverse ammonium-nitrogen flux was higher than 15 $g \cdot L^{-1}$, though the membrane used
306 was different (CTA-ES). These authors considered that data were too dispersed and that
307 it was difficult to obtain clear explanations. For water fluxes above 10 $L \cdot m^{-2} \cdot h^{-1}$, the
308 SRSF tended to the values that have been obtained in this work for the used membranes
309 under the described operating conditions.

310 Concerning to the brine, there were some differences in the SRSF depending on the ion.
311 It is relevant to note that the reverse flux of divalent cations was slightly lower for the
312 AIM than for the CTA-NW membrane. This could be explained by the positive charge
313 of the aquaporins [30] that would cause electrostatic repulsion with Ca^{+2} and Mg^{+2} ions.

However, the reverse flux of the rest of the ions was similar for both membranes. In general terms, it can be stated that the divalent ions of the draw solution had a similar behavior with both membranes in terms of SRSF, unlike the behavior showed when a sodium chloride solution was used as DS (Section 3.1).

When the reverse flux of each ion is compared, it seems clear that the lowest one is that measured for the sulfates as shown in Fig. 4.b. This is due to the fact that sulfate is the ion in the brine with the highest molecular size. The highest reverse flux corresponds to chloride (276 and 266 $mg \cdot L^{-1}$ for CTA-NW and AIM, respectively) due to the high chloride concentration in the DS (Fick´s law). The higher specific reverse flux of magnesium in comparison with calcium was due to its higher concentration in the brine.

Comparing the sulfate reverse flux in tests with both DS, it has to be commented that the values are very different because sulfate is the only significant anion in ALE. In this way, though the global SRSF for the same membrane could be practically constant, relevant differences among the specific reverse flux of the ions can be found.

a)

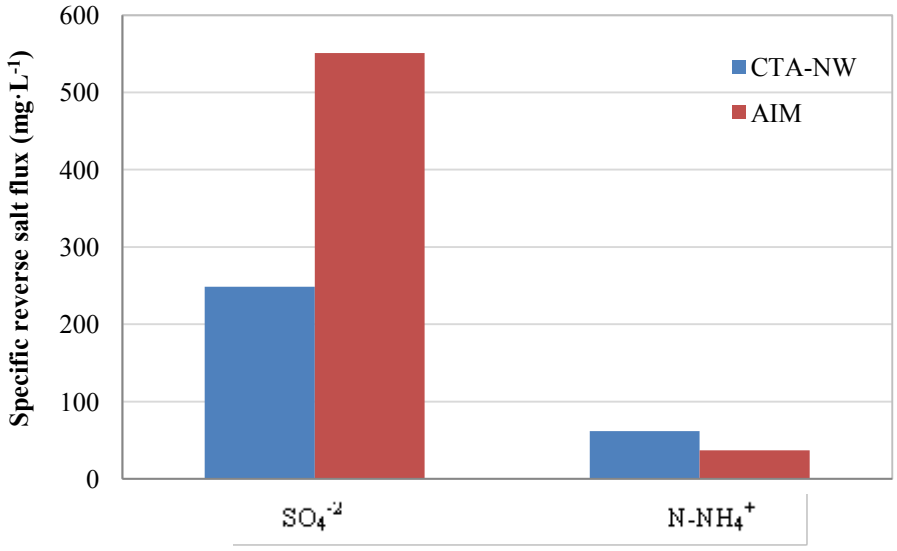

b)

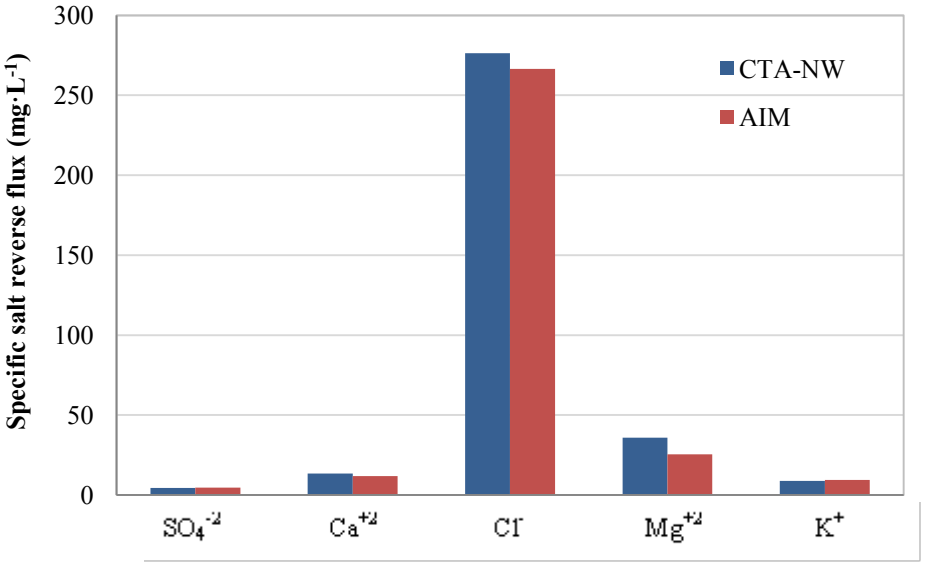

Figure 4: SRSF (mg·L^{-1}) of different ions in the experiments with deionized water as FS and a) ALE as DS and b) brine as DS.

340 3.3. Tests using anaerobically digested sludge centrate as feed solution

341 Permeate water flux and membrane fouling

342 Fig. 5 illustrates the change of permeate flux through time using ADSC as FS. It is clear
343 that the permeate flux decay is higher in comparison with that observed in the tests
344 using deionized water as FS (Fig. 3), which is due to the higher membrane active layer
345 fouling. In addition to it, in both tests with AIM there were time intervals in that
346 unexpected permeate water flux measurements were displayed. These tests were
347 repeated three times and a gradual decrease with the time (similar to that obtained for
348 CTA-NW membrane) was not obtained in either of them.

349 The active surface of the AIM membrane is characterized by the presence of aquaporins
350 or water channels (Fig. 6.a) whose size is lower than 250 nm. This in concordance with
351 Li et al. [31], who prepared TFC aquaporin-incorporated FO membranes, with vesicles
352 diameter around 100 nm (mean vesicle size). It is important to highlight the exacerbate
353 decrease and subsequent increase in AIM water flux when it was used brine as DS
354 around 50 h of operation time (Fig. 5.b). This anomalous behavior could be attributed to
355 the formation of a cake over the membrane surface. It seems as if the Aquaporin water
356 channels were blocked temporary, either by the organic matter of the ADSC or by
357 precipitated salts, and further they were back transported to the bulk solution and the
358 water flux was restored.

359 A sharp decline in permeate flux may be due to salts precipitation, as reported by
360 Phuntsho et al. [32], who observed a fast flux diminution processing brackish water as
361 FS and diamonnium phosphate as DS. The reverse phosphate flux caused magnesium
362 and calcium phosphates precipitation on the membrane feed side. Since permeate flux
363 was higher for AIM than for CTA-NW membrane, the highest reverse salt flux could

364 enhance the flux decay in the tests with the AIM membranes. Anyway, it has to be
365 commented that the final permeate flux measurements (after 72 h of operation) were the
366 highest in the tests with AIM for both DS. Zhang et al. [33] reported thoroughly the
367 calcium phosphate precipitation in FO processes. The flux decay trend reported by these
368 authors at a pH of 7.5 of the FS were very similar to our data with ADSC (pH = 8.1).

369 In order to corroborate salts precipitation, AIM membranes were observed after the tests
370 by FESEM (Fig. 6.b). The highlighted part in Fig. 6.b indicates the selected area
371 analyzed by EDX (Fig. 7). Fig. 6.b shows the membrane active layer after the test using
372 ADSC as FS and ALE as DS. Fouling was observed on the membrane active layer. The
373 square in the microphotography points out the area where the EDX was performed with
374 the aim of knowing the composition of the precipitates. This analysis is illustrated in
375 Fig. 7. It can be observed that P and Ca were the main elements determined on the
376 precipitates. It was due to calcium phosphate precipitation, since the solubility of this
377 compound in water is very low (25 $mg \cdot L^{-1}$ at 25ºC). As explained in section 2.1, the
378 concentration of calcium and phosphate in the effluent exiting the anaerobic digester is
379 high, which could produce a spontaneous precipitation at the exit of the anaerobic
380 digester in a wastewater treatment plant. The concentration of salts in ADSC is the same
381 as in the sludge at the digester exit; therefore it can be understood that an increase of
382 calcium and phosphate during the FO test may lead to calcium phosphate precipitation
383 due to concentration polarization at the surface of the membrane on the feed side.
384 Precipitation is expecting to occur at PO_4-P concentrations higher than 5 $mg \cdot L^{-1}$,
385 considering the above mentioned solubility. This implies a strong mass transfer
386 limitation [34]. In addition to it, S has been detected in the EDX analysis as it can be
387 observed in Fig.7. The presence of S on the active layer of the membrane was due to the

high reverse sulfates flux from the DS to the FS and the subsequent precipitation in the form of calcium sulfate over the membrane side in contact with FS.

a)

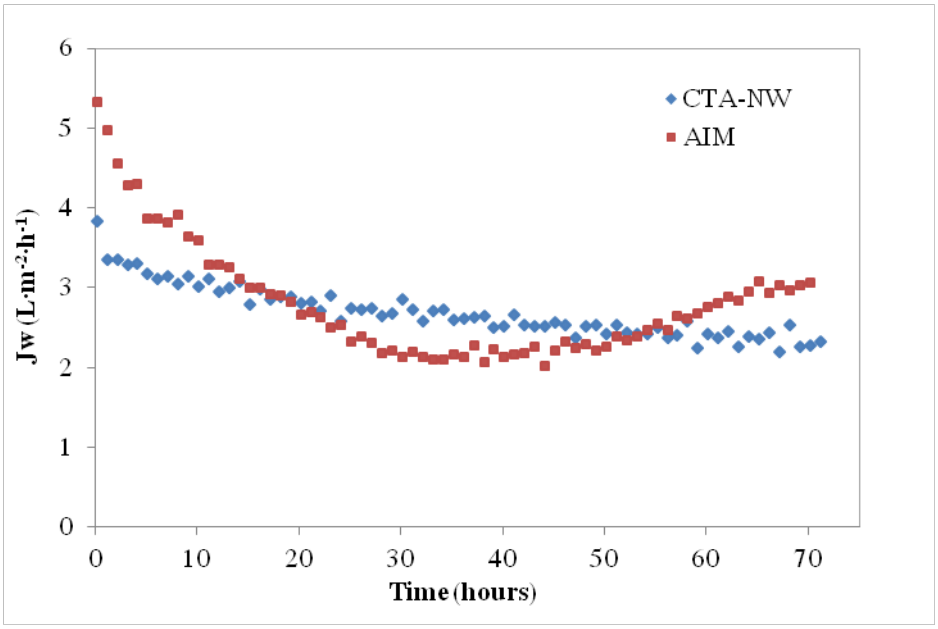

b)

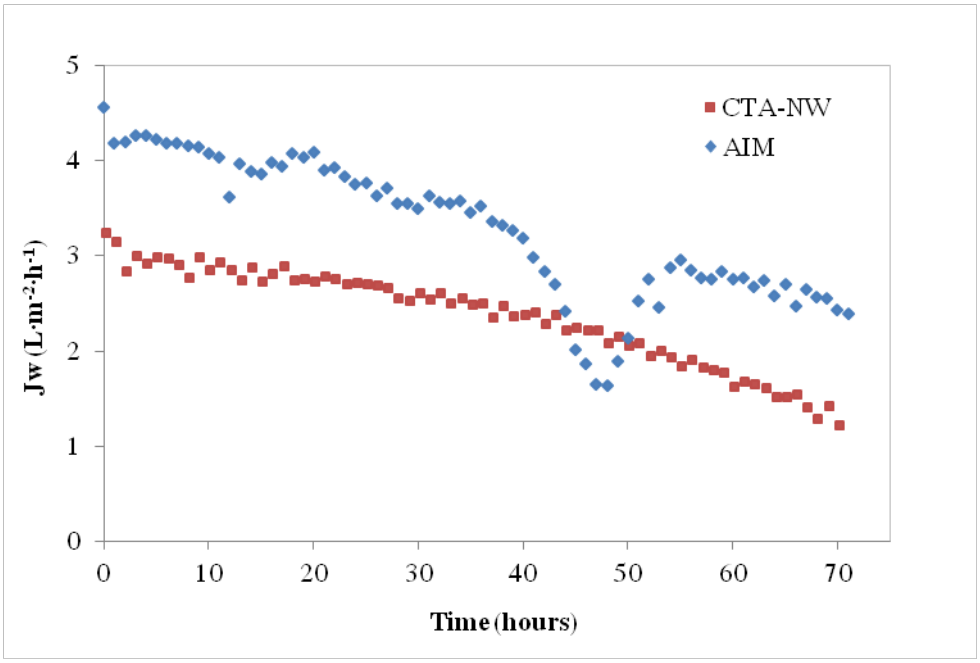

Figure 5: Flux evolution in the FO tests using ADSC as FS and a) ALE as DS and b) brine as DS.

a)

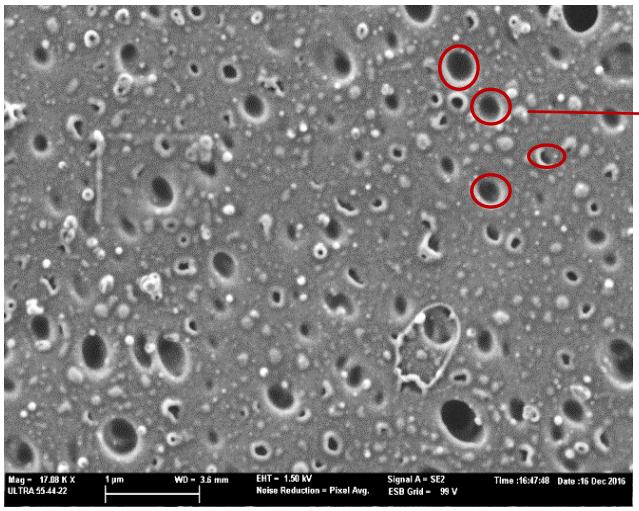

b)

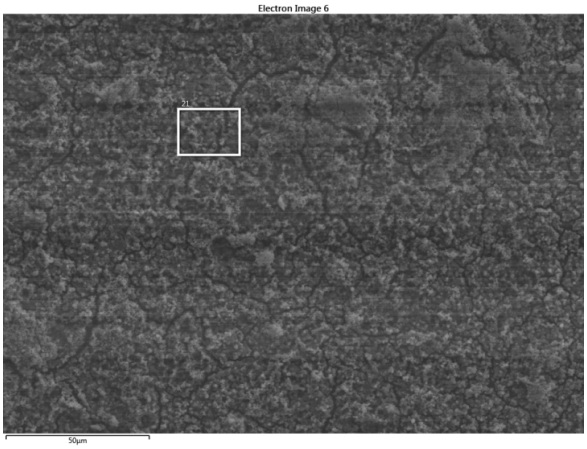

Figure 6: FE-SEM images: a) Water channels of the pristine active layer AIM membrane and b) AIM active layer after FO test (DS = ALE, FS = CADS).

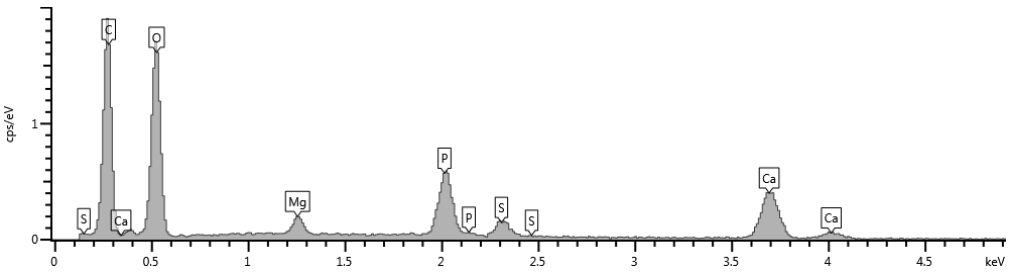

Figure 7: Analysis composition by EDX of the precipitates observed on AIM.

411 Nutrients recovery in the anaerobically digested sludge centrate

412 Table 5 shows the concentration of the TP and the ions measured at the beginning and
413 at the end of the 4 tests with ADSC. According to the results showed in Table 5, it is
414 clear that phosphorous cannot be concentrated in ADSC by means of FO. This is due to
415 its precipitation as calcium phosphate, which is corroborated by the measured calcium
416 concentration. Calcium concentration at the end of the tests using ALE as DS becomes
417 even lower than the initial one. This may be due to the enhancement of the calcium
418 precipitation by sulfate, since the reverse flux of this ion is very high, which is
419 explained by the Fick's law. In this way, both calcium phosphate and calcium sulfate
420 precipitates. This was corroborated in the EDX analysis as explained above (Fig. 7).
421 Summarizing, phosphate precipitation (which is clear especially for the most
422 concentrated ADSC in phosphate) avoids its recovery by FO when there is at the same
423 time a high calcium concentration. These results are in concordance with those reported
424 by Ansari et al. [7] who also observed spontaneous calcium phosphate precipitation.

425 Unlike phosphorous, ammonium nitrogen could be concentrated by FO. Table 6 shows
426 the main figures for understanding the ammonium nitrogen concentration in the tests. In
427 the first column, the volume exchanged between FS and DS can be observed. The
428 highest exchange volume correspond to the test in that no phosphorous precipitation
429 was observed (the TP concentration was higher at the end than at the beginning of the
430 test).

431 It can be observed that the expected ammonium nitrogen concentration is higher than
432 the measured one when brine was used as DS. This was due to the fact that there is no
433 ammonium nitrogen in the brine; therefore no reverse flux is possible. However, there is
434 passage of ammonium nitrogen through the membrane, since its rejection is not of

100%. In fact, it was calculated an ammonium rejection index of 83% for the CTA-NW and 66% for the AIM. On the contrary, the ammonium nitrogen concentration is much more efficient with the ALE than with the brine as DS. This is explained by the reverse ammonium flux, which concentrated the ammonium nitrogen in ADSC. In this way, the concentration factor (ratio between final and initial concentrations) of the ammonium nitrogen in the tests with ALE was 1.42 and 1.61 for CTA-NW and AIM, respectively.

Finally, if concentrations of monovalent ions are evaluated, it has to be commented that the reverse flux is much higher in the tests with brine, since concentrations of chloride, sodium and potassium are much higher in the brine than in ALE.

Table 5: Concentrations of the nutrients and ions in the ADSC (initial) and in the concentrated ADSC (final) at the end of the tests (all concentration are expressed in $mg \cdot L^{-1}$).

	CTA-NW DS = ALE		**CTA-NW DS = brine**		**AIM DS = ALE**		**AIM DS = brine**	
	initial	**final**	**initial**	**final**	**initial**	**final**	**initial**	**final**
TP	5.4	3.6	22	12	7	5	3	5
NH_4-N	824	1,172	922	992	655	1,055	928	1,086
SO_4^{2-}	110	215	120	170	60	320	45	110
Cl^-	1,260	1,620	1,640	2,260	900	1,340	1,560	2,380
Na^+	454	538	563	795	253	288	390	834
Ca^{2+}	345	245	205	227	180	120	200	220
Mg^{2+}	166	197	117	133	81	105	180	235
K^+	435	545	370	480	222	290	360	530

454 **Table 6: Ammonium nitrogen concentration in ADSC in the FO tests.**

Test	Volume from FS to DS (L)	Expected final NH_4-N concentration ($mg \cdot L^{-1}$)[1]	Measured final NH_4-N concentration ($mg \cdot L^{-1}$)	Concentration factor[2]
CTA-NW, DS = ALE	0.79	---	1,172	1.42
CTA-NW, DS = brine	0.79	1,207	992	1.08
AIM, DS = ALE	0.85	---	1,055	1.61
AIM, DS = brine	1.05	1,258	1,086	1.17

455 [1]**Assuming that there is no ammonium nitrogen reverse flux (in tests with brine) and that the membrane**
456 **rejection is 100%.**
457 [2] **Ratio between final and initial NH_4-N concentrations in ADSC.**
458

459

460 ## 4. Conclusions

461 In this paper, the recovery of nutrients in ADSC by FO using two actual industrial
462 effluents has been studied. The results showed higher permeate flux for the membrane
463 AIM than for the CTA-NW. Thus, the permeate water fluxes at the end of the experiments
464 with ALE as DS were 3.56 and 3.13 $L \cdot m^{-2} \cdot h^{-1}$ for the AIM and CTA-NW, respectively. The
465 final flux values in the experiments with brine as DS were 3.34 and 2.92 $L \cdot m^{-2} \cdot h^{-1}$ for
466 AIM and CTA-NW, respectively. These results also showed that using ALE is an
467 appropriate DS due to its high osmotic pressure.

468 Concerning the nutrients recovery, it can be concluded that nitrogen can be concentrated
469 in ADSC. On the contrary, phosphorous cannot be concentrated because of its
470 spontaneous precipitation as calcium phosphate during the FO process. In this way, a
471 previous controlled phosphate precipitation, for example using ferric chloride, is
472 proposed before the ADSC concentration by FO.

473 Unlike other works, actual industrial effluents have been used as draw solutions. On the
474 one hand, the use of the brine of a seawater desalination plant would drive to a

discharge of less concentrated brine to the sea. Obviously, it would be possible if the FO process for ADSC concentration would be carried out near the desalination plant. On the other hand, the use of the effluent from an absorption tower for ammonia removal enhanced the ammonium nitrogen concentration in ADSC due to its reverse flux in the FO process. The achieved concentration factor of the nitrogen using the new AIM was 1.61 when the ALE was used as DS.

Acknowledgments

This study was supported by the Spanish Ministry of Economy and Competitiveness through the project RTC-2015-3582-5-AR.

References

[1] R. Kumar, P. Pal, Turning hazardous waste into value-added products: Production and characterization of struvite from ammoniacal waste with new

approaches, J. Clean. Prod. 43 (2013) 59–70.

[2] M. Van den Berg, K. Neumann, D.P. Van Vuuren, A.F. Bouwman, T. Kram, J. Bakkes, Exploring resource efficiency for energy, land and phosphorus use: Implications for resource scarcity and the global environment, Glob. Environ. Chang. 36 (2016) 21–34.

[3] A.E. Ulrich, E. Frossard, On the history of a reoccurring concept: Phosphorus scarcity, Sci. Total Environ. 490 (2014) 694–707.

[4] T. Sölter, H. Orth, Stickstoffentfernung über Nitrit aus Trübwasser (Nitrogen elimination through nitrite from sludge water), Korrespondez Abwasser. 45 (1998), 1122-1131.

[5] A. Thornton, P. Pearce, S.A. Parsons, Ammonium removal from digested sludge liquors using ion exchange, Water Res. 41 (2007) 433–439.

[6] Y. Peng, L. Zhang, S. Zhang, Y. Gan, C. Wu, Enhanced nitrogen removal from sludge dewatering liquor by simultaneous primary sludge fermentation and nitrate reduction in batch and continuous reactors, Bioresour. Technol. 104 (2012) 144–149.

[7] A.J. Ansari, F.I. Hai, W.E. Price, L.D. Nghiem, Phosphorus recovery from digested sludge centrate using seawater-driven forward osmosis, Sep. Purif. Technol. 163 (2016) 1–7.

[8] R.W. Holloway, A.E. Childress, K.E. Dennett, T.Y. Cath, Forward osmosis for concentration of anaerobic digester centrate, Water Res. 41 (2007) 4005–4014.

[9] Q. Ping, Y. Li, X. Wu, L. Yang, L. Wang, Characterization of morphology and component of struvite pellets crystallized from sludge dewatering liquor: Effects of total suspended solid and phosphate concentrations, J. Hazard. Mater. 310 (2016) 261–269.

519 [10] U. Van Dongen, M.S.M. Jetten, M.C.M. Van Loosdrecht, The combined
520 Sharon/Anammox process. (2010). STOWA and IWA publishing, Padsrow, United
521 Kingdom.
522 [11] M.J. Vallés-Morales, J.A. Mendoza-Roca, A. Bes-Piá, A. Iborra-Clar, Nitrogen
523 removal from sludge water with SBR process: start-up of a full scale plant in the
524 municipal wastewater treatment plant at Ingolstadt, Water Sci. Technol. 50 (2004) 51–
525 58.
526 [12] C. Fux, S. Velten, V. Carozzi, D. Solley, J. Keller, Efficient and stable nitritation
527 and denitritation of ammonium-rich sludge dewatering liquor using an SBR with
528 continuous loading, Water Res. 40 (2006) 2765–2775.
529 [13] W. Xu, Q. Chen, Q. Ge, Recent advances in forward osmosis (FO) membrane:
530 Chemical modifications on membranes for FO processes, Desalination. 419 (2017)
531 101–116.
532 [14] L. Chekli, S. Phuntsho, J.E. Kim, J. Kim, J.Y. Choi, J.S. Choi, S. Kim, J.H. Kim,
533 S. Hong, J. Sohn, H.K. Shon, A comprehensive review of hybrid forward osmosis
534 systems: Performance, applications and future prospects, J. Memb. Sci. 497 (2016)
535 430–449. doi:10.1016/j.memsci.2015.09.041.
536 [15] B. Van der Bruggen, P. Luis, Forward osmosis: understanding the hype, Rev.
537 Chem. Eng. 31 (2015) 1–12.
538 [16] D.L. Shaffer, J.R. Werber, H. Jaramillo, S. Lin, M. Elimelech, Forward osmosis:
539 Where are we now?, Desalination. 356 (2015) 271–284.
540 [17] J. Duan, E. Litwiller, S.H. Choi, I. Pinnau, Evaluation of sodium lignin sulfonate
541 as draw solute in forward osmosis for desert restoration, J. Memb. Sci. 453 (2014) 463–
542 470.
543 [18] M.J. Luján-Facundo, J.L. Soler-Cabezas, J.A. Mendoza-Roca, M.C. Vincent-

544 Vela, A. Bes-Piá, A study of the osmotic membrane bioreactor process using a sodium
545 chloride solution and an industrial effluent as draw solutions, Chem. Eng. J. 322 (2017)
546 603–610.
547 [19] N.T. Hancock, T.Y. Cath, Solute Coupled Diffusion in Osmotically Driven
548 Membrane Processes, Environ.l Sci. Technol. 43 (2009) 6769–6775.
549 [20] W.A. Phillip, J.S. Yong, M. Elimelech, Reverse Draw Solute Permeation in
550 Forward Osmosis: Modeling and Experiments, Environ. Sci. Technol. 44 (2010) 5170–
551 5176.
552 [21] R.W. Holloway, R. Maltos, J. Vanneste, T.Y. Cath, Mixed draw solutions for
553 improved forward osmosis performance, J. Memb. Sci. 491 (2015) 121–131.
554 [22] S. Zou, M. Qin, Y. Moreau, Z. He, Nutrient-energy-water recovery from
555 synthetic sidestream centrate using a microbial electrolysis cell - forward osmosis
556 hybrid system, J. Clean. Prod. 154 (2017) 16–25.
557 [23] Y. Gao, Z. Fang, P. Liang, X. Huang, Direct concentration of municipal sewage
558 by forward osmosis and membrane fouling behavior, Bioresour. Technol. 247 (2018)
559 730–735.
560 [24] N. Martí, N., Barat, R., Seco, A., Pastor, L., Bouzas, Sludge management
561 modeling to enhance P-recovery as struvite in wastewater treatment plants, J. Environ.
562 Manag. 196 (2017) 340–346.
563 [25] APHA, AWWA, WEF, Standard Methods for the Examination of Water and
564 Wastewater., in: 21st ed., Washington, 2005.
565 [26] H.T. Nguyen, N.C. Nguyen, S.S. Chen, H.H. Ngo, W. Guo, C.W. Li, A new
566 class of draw solutions for minimizing reverse salt flux to improve forward osmosis
567 desalination, Sci. Total Environ. 538 (2015) 129–136.
568 [27] S. Zou, Z. He, Electrolysis-assisted mitigation of reverse solute flux in a three-

569 chamber forward osmosis system, Water Res. 115 (2017) 111–119.
570 [28] A. Tiraferri, N.Y. Yip, A.P. Straub, S. Romero-Vargas Castrillon, M. Elimelech,
571 A method for the simultaneous determination of transport and structural parameters of
572 forward osmosis membranes, J. Memb. Sci. 444 (2013) 523–538.
573 [29] H. Nasr, P. Sewilam, Investigating the performance of ammonium sulphate draw
574 solution in fertilizer drawn forward osmosis process, Clean Techn. Environ. Policy. 18
575 (2016) 717–727.
576 [30] P. Agre, D. Kozono, Aquaporin water channels: Molecular mechanisms for
577 human diseases, FEBS Lett. 555 (2003) 72–78.
578 [31] X. Li, C.H. Loh, R. Wang, W. Widjajanti, J. Torres, Fabrication of a robust
579 high-performance FO membrane by optimizing substrate structure and incorporating
580 aquaporin into selective layer, J. Memb. Sci. 525 (2017) 257–268.
581 [32] S. Phuntsho, F. Lotfi, S. Hong, D.L. Shaffer, M. Elimelech, H.K. Shon,
582 Membrane scaling and flux decline during fertiliser-drawn forward osmosis desalination
583 of brackish groundwater, Water Res. 57 (2014) 172–182.
584 [33] M. Zhang, Q. She, X. Yan, C.Y. Tang, Effect of reverse solute diffusion on
585 scaling in forward osmosis: A new control strategy by tailoring draw solution
586 chemistry, Desalination. 401 (2017) 230–237.
587 [34] R.W. Field, J.J. Wu, Mass transfer limitations in forward osmosis: Are some
588 potential applications overhyped?, Desalination. 318 (2013) 118–124.
589